09 Oct 2024

Protocol for Evaluating Anion Exchange Membranes for Nonaqueous Redox Flow Batteries

Jessica L. Tami

Md Motiur R. Mazumder

Grace E. Cook

Shelley D. Minteer
Missouri University of Science and Technology, shelley.minteer@mst.edu

et. al. For a complete list of authors, see https://scholarsmine.mst.edu/chem_facwork/4026

Recommended Citation

J. L. Tami et al., "Protocol for Evaluating Anion Exchange Membranes for Nonaqueous Redox Flow Batteries," *ACS Applied Materials and Interfaces*, vol. 16, no. 40, pp. 53643 - 53651, American Chemical Society, Oct 2024.
The definitive version is available at https://doi.org/10.1021/acsami.4c07026

ACS APPLIED MATERIALS & INTERFACES

www.acsami.org

Research Article

Protocol for Evaluating Anion Exchange Membranes for Nonaqueous Redox Flow Batteries

Jessica L. Tami, Md. Motiur R. Mazumder, Grace E. Cook, Shelley D. Minteer,* and Anne J. McNeil*

Cite This: *ACS Appl. Mater. Interfaces* 2024, 16, 53643−53651

Read Online

ACCESS | Metrics & More | Article Recommendations | Supporting Information

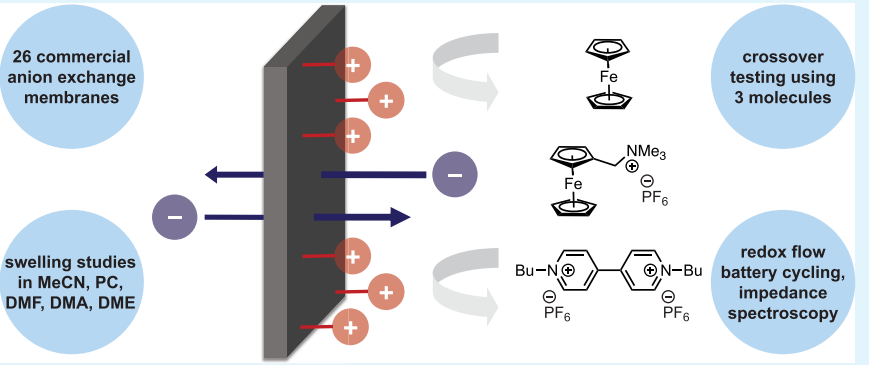

ABSTRACT: Nonaqueous redox flow batteries often suffer from reduced battery lifetime and decreased coulombic efficiency due to crossover of the redox-active species through the membrane. One method to mitigate this undesired crossover is to judiciously choose a membrane based on several criteria: swelling and structural integrity, size and charge of redox active species, and ionic conductivity. Most research to date has focused on reducing crossover by synthesizing modified redox-active molecules and/or new membranes. However, no standard protocol exists to compare membranes and a comprehensive study comparing membranes has yet to be done. To address both these limitations, we evaluate herein 26 commercial anion exchange membranes (AEMs) to assess their compatibility with common nonaqueous solvents and their resistance to crossover by using neutral and cationic redox-active molecules. Ultimately, we found that all the evaluated AEMs perform poorly in organic solvents due to uncontrolled swelling, low ionic conductivity, and/or high crossover rates. We believe that this method, and the generated data, will be useful to evaluate and compare the performance of all AEMs—commercial and newly synthesized—and should be implemented as a standard protocol for future research.

KEYWORDS: *anion exchange membranes, redox flow batteries, nonaqueous, crossover, permeability, electrochemical impedance spectroscopy, voltage efficiency*

INTRODUCTION

Renewable energy can be harvested through several avenues, including solar panels and wind turbines. However, solar and wind energy are intermittent, meaning they are not continuously accessible.[1] A safe, sustainable, and efficient way to store renewable energy is necessary so that it can be employed when needed. A promising technology for energy storage is the redox flow battery (RFB), which has the potential to be used in grid-scale operations.[2] RFBs consist of an electrochemical flow cell and two reservoirs, one of which contains an anolyte (redox-active species that undergoes reduction upon charging) and the other a catholyte (redox-active species that undergoes oxidation upon charging), both dissolved in a solvent with a supporting electrolyte (Scheme 1A).[3] An advantage to RFBs is that power and capacity can be independently scaled. Power is affected by the size of the electrodes (in each cell) and the number of cells whereas capacity is affected by the volume and concentration of redox-active molecules in the reservoirs.[4] The state-of-the-art commercial RFB is aqueous and uses expensive vanadium compounds for the redox-active molecules and hazardous sulfuric acid for the supporting electrolyte.[5−7] Additionally, aqueous batteries have a relatively small thermodynamic window (1.23 V) due to the hydrogen evolution reaction in reducing environments and the oxygen evolution reaction in oxidizing environments.[8] In contrast, nonaqueous RFBs (NARFBs) have a larger operating potential window (e.g.,

Received: May 7, 2024
Revised: September 12, 2024
Accepted: September 13, 2024
Published: September 30, 2024

Scheme 1. (A) RFB in Operation ; (B) AEM Impeding Positively Charged Redox-Active Species From Crossing Over

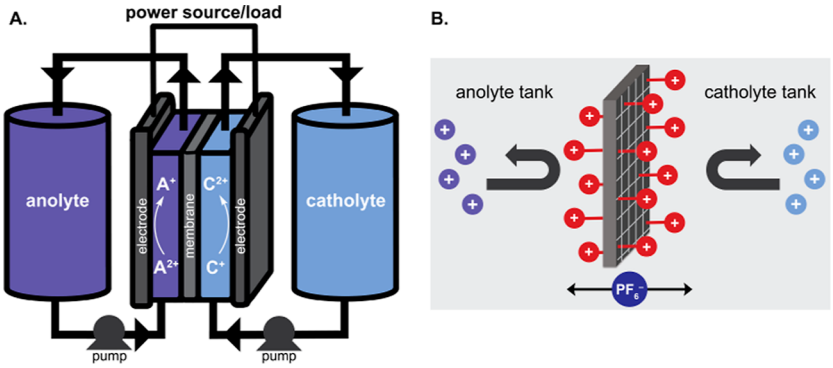

~5 V in acetonitrile), increasing the diversity of potential redox-active molecules, and enabling higher power densities as a result of larger attainable open circuit voltages.[9]

Between the two electrodes is a membrane or a separator, that functions to isolate the anolyte from the catholyte, preventing mixing (via crossover) of the redox-active molecules.[10] Crossover can occur through several mechanisms, including diffusion, osmosis, electroosmosis, and migration. Several membrane types have been used in RFBs, including polymers of intrinsic microporosity (PIMs), porous separators, ion-exchange membranes, and ceramic membranes.[11] Each type of membrane or separator caters to a specific system. For example, PIMs offer size exclusion, which is advantageous when working with oligomeric or polymeric redox-active materials.[12,13] Porous separators such as Daramic or Celgard, have been frequently used in NARFBs due to their relatively high ionic conductivity, which enables battery cycling at higher current densities.[14−16] However, this improved conductivity comes at the expense of high crossover rates, especially with small redox-active species. The result is lower coulombic efficiencies and lifetimes of the battery.

One method to decrease crossover is to use a premixed symmetric flow cell wherein equal quantities of anolyte and catholyte are dissolved in each reservoir,[17,18] but doing so effectively wastes half of the redox-active materials. Additionally, there will still be a concentration gradient of the electrochemically charged species across the cell during cycling, so crossover may still occur, and coulombic efficiency will suffer. A technologically relevant battery (i.e., a battery with high capacity, energy density, and energy efficiency) will be nonsymmetric and have a membrane that is both highly conductive and prevents crossover.

Commercial ion-exchange membranes were originally fabricated for aqueous systems, such as fuel cells, water purification, desalination, dialysis, and/or aqueous RFBs.[19−21] Specifically, AEMs are cross-linked polymers, assembled into three-dimensional networks with fixed, ionic functional groups (i.e., $-NH_3^+$, $-NRH_2^+$, $-NR_2H^+$, $-NR_3^+$, and $-SR_2^+$).[19] AEMs should repel positively charged molecules, ensuring that cationic molecules stay in their respective tank.[22] In AEMs, only anionic supporting electrolyte ions, like PF_6^- or BF_4^-, can traverse the membrane for charge balancing during charging and discharging (Scheme 1B). AEMs have been used in nonaqueous, inorganic RFBs for decades[23−26] but have more recently been adopted in nonaqueous organic RFBs. For instance, Sanford and co-workers used an AEM in organic NARFBs (Fumasep FAP-375-PP) to mitigate the crossover of redox-active cyclopropenium species.[12,27−29] Increasing charge incorporation and molecular size decreased the rate of crossover, with a tetramer (4^+ charge) crossing over so slowly it was below the limit of detection within the time frame of their experiment. As a result, FAP-375-PP has been the go-to commercial membrane in many nonaqueous RFB studies,[31] in addition to FAPQ-375-PP.[30,32−33] However, both FAP-375-PP and FAPQ-375-PP have been discontinued by the manufacturer.

To date, a systematic study has not directly compared AEMs,[30,34−39] so it is unclear what membranes would perform best in flow battery systems. To address this limitation, we evaluated herein 26 AEMs (Table 1) for structural stability in electrochemically relevant organic solvents. From these results, seven membranes were selected for further evaluation, including measuring crossover rates, ionic conductivities, and performance in a RFB. Overall, these data reveal that most commercial AEMs do not perform satisfactorily in lab-scale NARFBs. Moving forward, we suggest that researchers developing new membranes and/or evaluating new commercial membranes utilize the standard protocol described herein for benchmarking and comparison.

Table 1. Commercial AEMs Evaluated

Fumasep		Sustainion
FAP-330	FAB-PK-130	E30-50, T
FAPQ-330	FAD-55	E28-50, T
FAP-450	FAS-30	B22-50, T
FAA-3-30	FAS-50	X37-50, RT
FAA-3-50	FAP-330-PE	X37-50, T
FAPQ-375-PP	FAD-PET-75	**PiperION**
FAA-3-PK-75	FAS-PET-75	15 μm PTFE
FAA-3-PK-130	**AMI-7001S**	20 μm
FAM	**AEMION+**	80 μm

(Color Blocks Indicate Different Manufacturers of AEMs)

RESULTS AND DISCUSSION

Most Commercial AEMs Dissolve or Deform in Nonaqueous Solvents. All membranes were first pretreated in a saturated, aqueous solution of potassium hexafluorophosphate (KPF_6) to exchange the mobile counterions in the polymer resin with PF_6^- anions to match the supporting electrolyte used in crossover and battery studies (see Supporting Information for examples with NH_4PF_6 pretreatment). After drying, the membranes were cut into small

https://doi.org/10.1021/acsami.4c07026
ACS Appl. Mater. Interfaces 2024, 16, 53643−53651

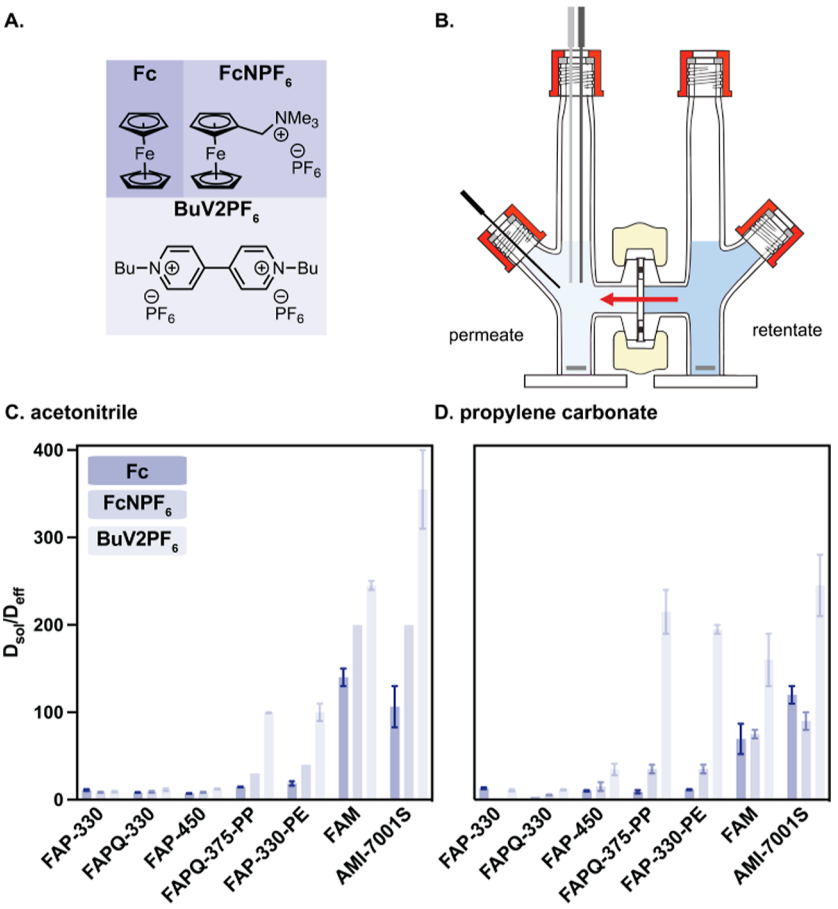

Figure 1. (A) Structures of catholytes and anolyte. (B) H-cell used for crossover experiments, adapted from Adams & Chittenden Scientific Glass Coop.[46] (C) Plot of membrane performance (D_{sol}/D_{eff}) in 0.5 M KPF_6 in MeCN. (D) Plot of membrane performance in 0.1 M KPF_6 in PC. All bars represent the average of two trials. The error bars represent the range of values.

rectangles for further analysis. To qualitatively assess the membranes' structural stability, the AEMs were soaked in neat organic solvent (MeCN, PC, DMF, DMA, and DME, separately) for 48 h to simulate long-term cycling conditions. Every membrane deformed in DMF and DMA, either dissolving completely or swelling excessively after soaking, even those with mechanical reinforcements (i.e., a polymer support). Too much swelling will immediately allow redox species to crossover the membrane.[11,40] In contrast, many membranes remained intact in DME, but some turned opaque, which is likely caused by a change in polymer properties (e.g., solubility). Photos of all ion-exchanged AEMs taken before and after soaking in organic solvents are included in the Supporting Information (Section SIII).

Both MeCN and PC were chosen as the organic solvents for subsequent studies due to the incompatibility of AEMs in DMF and DMA, and the low relative permittivity of DME.[41] Additionally, PC and MeCN are the two most widely used solvents in the NARFB field. Acetonitrile is an ideal organic solvent in NARFBs because of its large electrochemical window and high dielectric permittivity. Propylene carbonate is considered a green solvent because of its low relative toxicity and environmental impact, making it attractive for commercial applications.[42] However, PC does have some drawbacks, such as a higher viscosity and lower conductivity than comparable electrolytes in MeCN. Among the 26 commercial AEMs examined, only seven demonstrated stability (no dissolution or deformation) in MeCN and PC: FAP-330, FAPQ-330, FAP-450, FAPQ-375-PP, FAP-330-PE, FAM, and AMI-7001S. These membranes were analyzed for increases in length, width, thickness, and mass to measure swelling from solvent uptake (see Section SIII of the Supporting Information). Interestingly, of the three membranes that swelled the least in MeCN and PC, only one (FAM) included a mechanical support (a polypropylene mesh). These results suggest that these mechanical reinforcements do not prevent swelling in nonaqueous solvents (see Supporting Information Figure S4).

Too Much Membrane Swelling Leads to Higher Permeability. Crossover rates were measured for three different redox-active small molecules with increasing positive charges: neutral ferrocene (Fc, catholyte), monocationic (1^+) ammonium-appended ferrocene ($FcNPF_6$, catholyte), and dicationic (2^+) butyl viologen ($BuV2PF_6$, anolyte) (Figure 1A). These molecules were chosen because they are electrochemically stable to galvanostatic cycling and are commercially available or easily synthesized. Additionally, these molecules have similar hydrodynamic radii (molecular size in solution),[43] so conclusions regarding crossover rates can be made primarily based on charge interactions with the positively charged membrane instead of size-exclusion. An H-cell was used for crossover studies,[44] enabling the membrane to sit between two-half cells: one, the retentate, is composed of 25 mM redox-active material in supporting electrolyte and solvent (either 0.5 M KPF_6 in MeCN or 0.1 M KPF_6 in PC) and the other, the permeate, only contains supporting electrolyte in solvent (Figure 1B). A lower concentration of supporting electrolyte

https://doi.org/10.1021/acsami.4c07026
ACS Appl. Mater. Interfaces 2024, 16, 53643−53651

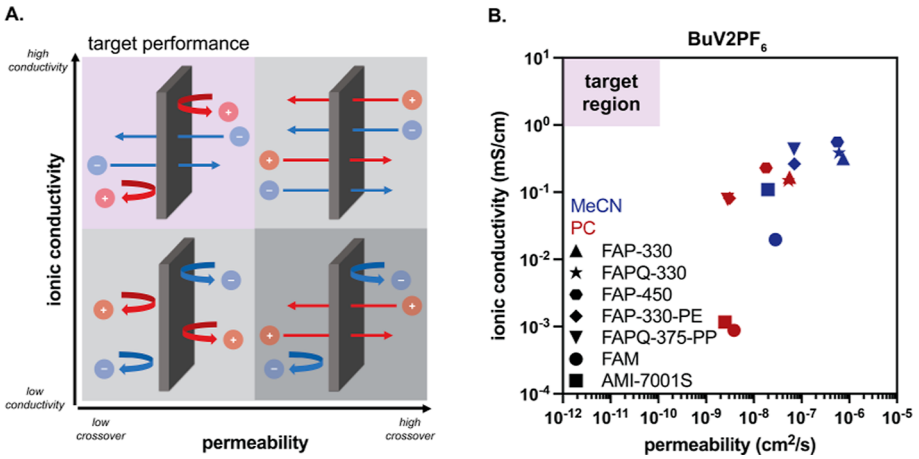

Figure 2. (A) Idealized plot of ionic conductivity of supporting electrolyte anions and permeability of redox-active cations through AEMs. (B) Plot of measured ionic conductivity and permeability of each AEM in MeCN and PC with $BuV2PF_6$.

was used in PC due to the low solubility of KPF_6. Note that the supporting electrolyte concentrations were adjusted so that the ionic strengths were the same in both reservoirs. Crossover was monitored by cyclic voltammetry, which relates measured peak current to the concentration of redox-active material using a three-electrode setup on the permeate side of the H-cell. In these experiments, redox-active species diffusion through the membrane is being measured; osmosis and electroosmosis are unlikely contributors to the crossover because solvent imbalances were not observed. Though not used in this study, ultraviolet−visible (UV−vis) and nuclear magnetic resonance (NMR) spectroscopy are also viable methods of measuring crossover.[45]

Each membrane has a different thickness, and each molecule has a different diffusion coefficient in solution. Therefore, to compare results between membranes and molecules, we used the ratio between the redox-active molecule's diffusion coefficient in the electrolyte (D_{sol}) and its effective diffusion, or permeability, through the membrane (D_{eff}). Specifically, we used the Randles−Ševčík equation to calculate D_{sol}[47,48] (Supporting Information Section SVII) and the following equation, derived from Fick's laws of diffusion, for D_{eff}[49] (Supporting Information Section SVIII)

$$D_{eff} = \frac{C_{permeate} \times l \times V_{permeate}}{C_0 \times A}$$

$C_{permeate}$ is the initial rate of crossover (mol/s·cm^3), l is the thickness of the dry membrane (cm), $V_{permeate}$ is the volume of the permeate (cm^3), C_0 is the initial redox material concentration on the retentate side (mol/cm^3), and A is the area of the membrane exposed to solution (cm^2).

Both the absolute value and the relative values of D_{sol}/D_{eff} between molecules are important measurements. A higher absolute value of D_{sol}/D_{eff} equates to a better membrane blocking ability, whereas the relative values between the redox-active molecules studied herein reflect the membranes' selectivity for repelling positively charged molecules.[13] We want to highlight that D_{eff} is the product of redox species diffusion through the membrane (transport) and absorption (e.g., partitioning through the membrane), which is a thermodynamic process. Active species transport is important in flow cell cycling and can affect capacity fade, particularly in less conductive membranes, but it is not the sole contributor to permeability.

In MeCN, FAM and AMI-7001S are the best at suppressing crossover of all molecules. Both membranes display charge selectivity because they suppress the dication ($BuV2PF_6$) better than the monocation ($FcNPF_6$), and the monocation better than neutral compound (Fc) (Figure 1C). Though these two AEMs have the slowest crossover rates, they also have the lowest ionic conductivities and would therefore require a large overpotential to run in a NARFB (vide infra).

In PC, the most ion-selective membranes were FAPQ-375-PP and FAP-330-PE, both of which dramatically suppress the crossover of the dication compared to the monocation and neutral molecule (Figure 1D). These membranes, however, have both been discontinued from commercial suppliers. FAM and AMI-7001S also performed well comparatively but again suffered from low ionic conductivity (vide infra). Permeability (D_{eff}) should be no higher than 10^{-10} cm^2/s and the lowest (slowest) value obtained in this work was 10^{-8} cm^2/s for FAM and AMI-7001S in PC, a factor of 10^2 faster, meaning that even the best performers in our study could never be commercially viable.[40]

Though we cannot attribute performance to the membranes' chemical structure, which is proprietary, we observe a "Goldilocks" correlation between solvent uptake and membrane performance in the limited data (7 membranes; Figure S4). Membranes with a high solvent uptake generally have more crossover (i.e., a smaller D_{sol}/D_{eff} value.) For example, the weight of FAP-330 increased by 327% after soaking in MeCN and is a poor membrane with respect to crossover (D_{sol}/D_{eff} of 9.4 for $BuV2PF_6$). Similarly, membranes with a low solvent uptake also showed more crossover. For example, FAPQ-330 had a mass gain of only 8% in MeCN and had an average D_{sol}/D_{eff} of 11 with $BuV2PF_6$. In contrast, the membranes with "in between" mass gains showed the least crossover. For example, FAM and AMI-7001S exhibited a more moderate weight increase of 24% and 31%, respectively, and have the best crossover performance (D_{sol}/D_{eff} of 240 and 360 for $BuV2PF_6$, respectively) in MeCN (Supporting Information Table S2).

AEMs with the Least Crossover Have the Lowest Ionic Conductivity. AEMs should be tested in a flow battery for a more accurate comparison to grid-scale applications. As such, flow batteries were run using cationic $FcNPF_6$ as the

https://doi.org/10.1021/acsami.4c07026
ACS Appl. Mater. Interfaces 2024, 16, 53643−53651

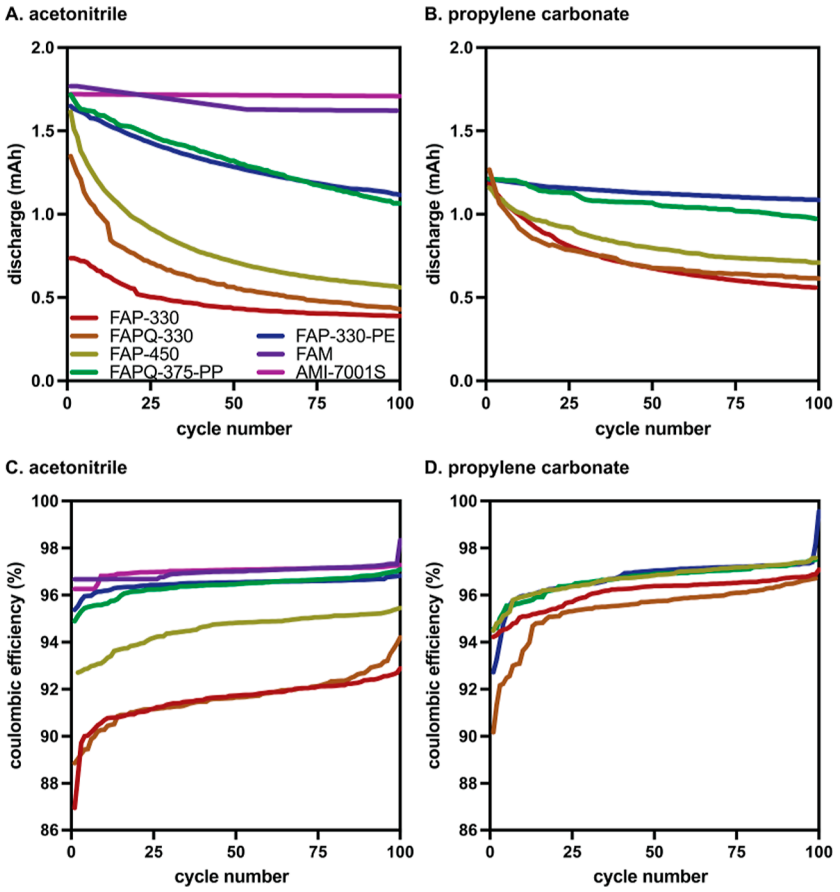

Figure 3. Capacity fade in (A) MeCN and (B) PC. coulombic efficiency in (C) MeCN and (D) PC over 100 cycles. The theoretical capacity of the battery is 2.7 mAh.

Table 2. Dry Thickness, Ionic Conductivity, and Voltage Efficiency Values for AEMs in MeCN and PC

		ionic conductivity (μS/cm)		voltage efficiency (%)	
AEM	dry thickness (μm)	MeCN	PC	MeCN	PC
FAP-330	32	317 ± 7	168 ± 4	87 ± 1	80 ± 1
FAPQ-330	36	390 ± 10	151 ± 3	90 ± 1	74 ± 1
FAP-450	56	560 ± 10	231 ± 4	95 ± 1	78 ± 1
FAPQ-375-PP	107	440 ± 10	78 ± 3	90 ± 1	34 ± 1
FAP-330-PE	45	263 ± 8	81 ± 1	95 ± 1	66 ± 1
FAM	526	19.7 ± 0.03	0.88 ± 0.03	21.0 ± 0.5	n.d
AMI-7001S	568	110 ± 3	1.17 ± 0.05	33.5 ± 0.5	n.d

catholyte and dicationic BuV2PF$_6$ as the anolyte, with either 0.5 M KPF$_6$ in MeCN or 0.1 M KPF$_6$ in PC. High ionic conductivity through the membranes is critical for AEMs in a flow cell to complete the circuit and balance charge efficiently. Ionic conductivity is an intrinsic property of membranes in supporting electrolytes, and, in our study, is measured via electrochemical impedance spectroscopy (EIS), though it could also be measured with a four-point probe.[50] Ions can move through the membrane as solvated ions, solvent-separated ion pairs, contact ion pairs, or in aggregates. Because the batteries used low-to-moderate ion concentrations, and the membranes were swollen, we expect that the ions primarily move through the membranes as solvated free ions, though the other mechanisms are possible.[51,52]

The system resistance was calculated by subtracting the bulk electrolyte resistance (measured from a blank experiment without a membrane) from the total resistance measured in the flow cell. For AEMs in nonaqueous systems, a practical ionic conductivity range is > 1 mS/cm by way of the maximum area-specific resistance for a membrane with a thickness of ~25 μm (2.3 $\Omega \cdot cm^2$).[53,54] None of the membranes exhibited ionic conductivities over 1 mS/cm (Table 1 and Figure S5). Membranes with high ionic conductivity and low redox-active molecule permeability are desired (Figure 2A). Unfortunately, the membranes with the highest ionic conductivities also exhibited the highest permeabilities of redox-active species (Figure 2B). These results cannot be explained by differences in swelling (Figure S6); as an example, the least (8%) and most (327%) swollen membranes both exhibited similar ionic conductivities (317 and 390 μS/cm, respectively) and permeabilities (7.43×10^{-7} and 6.12×10^{-7} cm^2/s; for BuV2PF$_6$ in MeCN). Overall, the data show that no membrane, solvent, or redox molecule combination was able

https://doi.org/10.1021/acsami.4c07026
ACS Appl. Mater. Interfaces 2024, 16, 53643−53651

Scheme 2. Recommended Protocol for Evaluating the Performance of AEMs

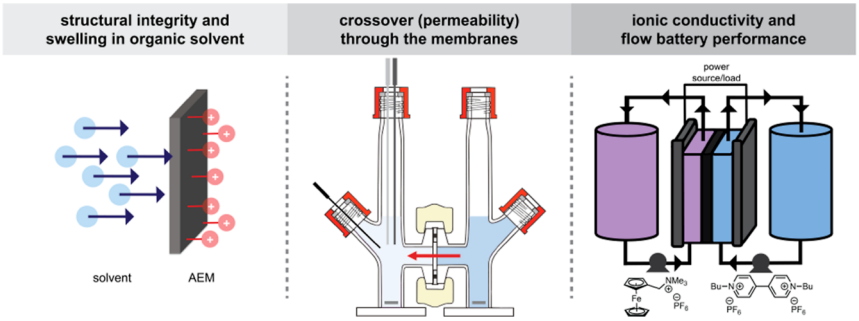

to reach these targeted metrics, and as a result, none of the evaluated systems are suitable for NARFB applications.

Nevertheless, all seven membranes were advanced to battery testing to measure capacity fade, coulombic efficiency, and voltage efficiency, among other variables. Capacity fade measures how much redox-active material can be discharged over time, with a lower fade equating to a longer battery lifetime.[55] Coulombic efficiency is the difference between the capacities reached during charging and discharging and reflects how much of stored charge is accessible. Voltage efficiency accounts for any overpotential necessary to run the battery and dictates whether enough power is generated to be commercially viable. Ideally, a battery will have low capacity fade, high coulombic efficiency, and high voltage efficiency. However, it can be challenging to simultaneously optimize these factors in RFBs.

In MeCN, the membranes with the lowest capacity fade and the highest coulombic efficiency were FAM and AMI-7001S (Figure 3). However, both FAM and AMI-7001S have low voltage efficiencies (34% and 21%, respectively) (Table 2), requiring considerably more energy to run the battery than the open-circuit voltage (1.05 V). In PC, the best membrane was FAP-330-PE, which had the lowest capacity fade (10% over 22 h), with a high coulombic efficiency (97%) and modest voltaic efficiency (80%).[56] Nevertheless, this membrane was discontinued and is no longer available. The capacity fade is likely due to crossover due to both diffusion and migration, which may explain why the discharge capacity surpasses 50% losses in FAP-330, FAPQ-330, and FAP-450.[57,58] No solvent imbalances were observed, suggesting that neither osmosis nor electroosmosis contributed to crossover.

A Standardized Protocol is Necessary to Compare Between Commercial and Synthesized Membranes. If all studies use the same redox-active molecules, solvents, and supporting electrolytes for crossover and battery testing, a direct comparison can be made between different membranes. To this end, we recommend that all NARFB groups that are synthesizing their own AEMs (or evaluating new commercial membranes) use the following protocol as a baseline: (1) membrane integrity testing and swelling measurements in MeCN, PC, DMF, DMA, and DME, (2) crossover studies using Fc, $FcNPF_6$, and $BuV2PF_6$, (3) EIS to determine ionic conductivity, and (4) flow battery cycling.

To maximize ionic conductivity of supporting electrolyte (e.g., KPF_6), we suggest using MeCN as a solvent over PC, assuming similar redox-active molecule solubility in both solvents. KPF_6 is a convenient supporting electrolyte because it has no ^1H or ^{13}C signals via NMR spectroscopy, simplifying spectral analyses that may provide insight into redox-active molecule degradation. If this protocol is widely adopted, it will be easier to benchmark membranes and push the boundaries of membrane fabrication for RFBs.

Limitations and Other Considerations. Our workflow focuses on the membranes, and an easily translatable performance test to benchmark them. Initially, structural integrity and swelling of AEMs is evaluated (Scheme 2, left) followed by permeability of redox molecules through the membranes (Scheme 2, center), and finally flow battery performance and ionic conductivity (Scheme 2, right). However, some conditions must be considered when adopting our methodology. Although Fc, $FcNPF_6$, and $BuV2PF_6$ are good model compounds, we recognize that crossover can also be mitigated through chemical synthesis (i.e., installing ionic functional groups onto redox molecules to be repelled by ion exchange membranes), meaning that our measured crossover rates of neutral, 1^+, and 2^+ species may not translate perfectly to other molecules.

Additionally, some membrane characterization methods (i.e., ion-exchange capacity,[59] swelling/sorption with different supporting electrolytes,[60] and surface area/pore size of the membrane[61]) lie beyond the scope of this study but are important for full characterization of new membranes. Other methods to evaluate electrochemical performance and crossover in situ include dialysis diagnostics using an applied electric field by Darling and co-workers[62] and compositionally unbalanced symmetric cell cycling by Brushett and co-workers.[63]

Furthermore, our protocol is performed at low concentrations but transport and membrane properties (i.e., conductivity, partitioning, swelling) are likely to change at application-relevant active species concentrations.[64] Battery performance depends on volume, flow rate, concentrations of redox species, viscosity, electrode area, temperature, battery cell structure, and many other parameters. With these considerations, we emphasize that this study is for membrane comparison, and the relative values between the model compounds and membranes are what enable a precise comparison.

CONCLUSIONS

Commercially available AEMs were examined as potential membranes for NARFBs. Performance was compared based on structural stability in nonaqueous solvents, swelling, crossover of the redox-active molecules, ionic conductivity , and a 100-cycle flow battery. Of the 26 membranes initially tested, only seven membranes emerged as good candidates for full evaluation. Overall, no commercial AEM studied had an acceptable performance in all categories. Based on our data,

https://doi.org/10.1021/acsami.4c07026
ACS Appl. Mater. Interfaces 2024, 16, 53643−53651

FAPQ-375-PP and FAP-330-PE are the best membrane candidates for nonaqueous RFBs in acetonitrile and only the latter membrane works well in propylene carbonate; however, these two membranes have been discontinued by the manufacturer. Consequently, new membranes (commercial or synthesized[65−68]) are needed for NARFBs and should be evaluated using our suggested protocol to accurately benchmark them against existing membranes.

■ ASSOCIATED CONTENT

Supporting Information

The Supporting Information is available free of charge at https://pubs.acs.org/doi/10.1021/acsami.4c07026.

All materials, synthetic and electrochemical procedures, structural (NMR, MS, and elemental analysis) and electrochemical characterization (crossover, CV, EIS, batteries), solvent uptake and swelling studies, and photos of all AEMs in organic solvents are provided in the Supporting Information (PDF)

■ AUTHOR INFORMATION

Corresponding Authors

Shelley D. Minteer − *Department of Chemistry, Missouri University of Science and Technology, Rolla, Missouri 65409-6518, United States; Kummer Institute Center for Resource Sustainability, Missouri University of Science and Technology, Rolla, Missouri 65409-6518, United States;* Email: shelley.minteer@mst.edu

Anne J. McNeil − *Department of Chemistry, University of Michigan, Ann Arbor, Michigan 48109-1055, United States; Macromolecular Science and Engineering Program, University of Michigan, Ann Arbor, Michigan 48109-1055, United States;* orcid.org/0000-0003-4591-3308; Email: ajmcneil@umich.edu

Authors

Jessica L. Tami − *Department of Chemistry, University of Michigan, Ann Arbor, Michigan 48109-1055, United States;* orcid.org/0000-0003-3106-5790

Md. Motiur R. Mazumder − *Department of Chemistry and Biochemistry, Utah Tech University, St. George, Utah 84770-3875, United States*

Grace E. Cook − *Department of Chemistry, University of Michigan, Ann Arbor, Michigan 48109-1055, United States;* orcid.org/0009-0008-2154-6455

Complete contact information is available at: https://pubs.acs.org/10.1021/acsami.4c07026

Author Contributions

CRediT: **Jessica L. Tami** contributed to conceptualization (equal), data curation (equal), formal analysis (equal), methodology (equal), visualization (lead), writing original draft (lead), and writing review and editing (lead). **Md. Motiur R. Mazumder** contributed to conceptualization (equal), data curation (equal), formal analysis (equal), and methodology (equal). **Grace E. Cook** contributed to data curation and methodology. **Shelley D. Minteer** contributed to conceptualization, funding acquisition, investigation, project administration, resources, supervision, and writing review and editing. **Anne J. McNeil** contributed to conceptualization, funding acquisition, investigation, project administration, resources, supervision, and writing review and editing.

Funding

This research was supported by the Department of Energy through the Joint Center for Energy Storage Research (JCESR), an Energy Innovation Hub funded by the U.S. Department of Energy, Office of Science, Basic Energy Sciences.

Notes

The authors declare no competing financial interest.

■ ACKNOWLEDGMENTS

J.L.T., M.M.R.M., A.J.M. and S.D.M. gratefully acknowledge support and helpful conversations from the Joint Center for Energy Storage Research. J.L.T. and A.J.M. thank Dr. Bertrand Neyhouse, the Sanford Group, and Prof. Melanie Sanford for helpful discussions.

■ ABBREVIATIONS

AEM	anion exchange membrane
Fc	ferrocene
RFB	redox flow battery
NARFB	nonaqueous redox flow battery
MeCN	acetonitrile
PC	propylene carbonate
DMF	*N*,*N*-dimethylformamide
DMA	*N*,*N*-dimethylacetamide
DME	dimethoxyethane
ASR	area specific resistance
NMR	nuclear magnetic resonance spectroscopy
UV−vis	ultraviolet−visible spectroscopy
OCV	open circuit voltage
EIS	electrochemical impedance spectroscopy

■ REFERENCES

(1) Ziegler, M. S.; Mueller, J. M.; Pereira, G. D.; Song, J.; Ferrara, M.; Chiang, Y.-M.; Trancik, J. E. Storage Requirements and Costs of Shaping Renewable Energy Toward Grid Decarbonization. *Joule* **2019**, *3*, 2134−2153.

(2) Sánchez-Díez, E.; Ventosa, E.; Guarnieri, M.; Trovò, A.; Flox, C.; Marcilla, R.; Soavi, F.; Mazur, P.; Aranzabe, E.; Ferret, R. Redox Flow Batteries: Status and Perspective Towards Sustainable Stationary Energy Storage. *J. Power Sources* **2021**, *481*, 228804.

(3) Noack, J.; Roznyatovskaya, N.; Herr, T.; Fischer, P. The Chemistry of Redox-Flow Batteries. *Angew. Chem., Int. Ed.* **2015**, *54*, 9776−9809.

(4) Arévalo-Cid, P.; Dias, P.; Mendes, A.; Azevedo, J. Redox Flow Batteries: A New Frontier on Energy Storage. *Sustainable Energy Fuels* **2021**, *5*, 5366−5419.

(5) Choi, C.; Kim, S.; Kim, R.; Choi, Y.; Kim, S.; Jung, H.; Yang, J. H.; Kim, H.-T. A Review of Vanadium Electrolytes for Vanadium Redox Flow Batteries. *Renewable Sustainable Energy Rev.* **2017**, *69*, 263−274.

(6) Lourenssen, K.; Williams, J.; Ahmadpour, F.; Clemmer, R.; Tasnim, S. Vanadium Redox Flow Batteries: A Comprehensive Review. *J. Energy Storage* **2019**, *25*, 100844.

(7) Cunha, Á.; Martins, J.; Rodrigues, N.; Brito, F. P. Vanadium Redox Flow Batteries: A Technology Review. *Int. J. Energy Res.* **2014**, *39*, 889−918.

(8) Kühnel, R.-S.; Reber, D.; Battaglia, C. Perspective−Electrochemical Stability of Water-in-Salt Electrolytes. *J. Electrochem. Soc.* **2020**, *167*, 070544.

(9) Li, M.; Rhodes, Z.; Cabrera-Pardo, J. R.; Minteer, S. D. Recent Advancements in Rational Design of Non-Aqueous Organic Redox Flow Batteries. *Sustainable Energy Fuels* **2020**, *4*, 4370−4389.

(10) Huang, Y.; Gu, S.; Yan, Y.; Li, S. F. Y. Nonaqueous Redox-Flow Batteries: Features, Challenges, and Prospects. *Curr. Opin. Chem. Eng.* **2015**, *8*, 105−113.
(11) Yuan, J.; Pan, Z.-Z.; Jin, Y.; Qiu, Q.; Zhang, C.; Zhao, Y.; Li, Y. Membranes in Non-Aqueous Redox Flow Battery: A Review. *J. Power Sources* **2021**, *500*, 229983.
(12) Hendriks, K. H.; Robinson, S. G.; Braten, M. N.; Sevov, C. S.; Helms, B. A.; Sigman, M. S.; Minteer, S. D.; Sanford, M. S. High-Performance Oligomeric Catholytes for Effective Macromolecular Separation in Nonaqueous Redox Flow Batteries. *ACS Cent. Sci.* **2018**, *4*, 189−196.
(13) Doris, S. E.; Ward, A. L.; Baskin, A.; Frischmann, P. D.; Gavvalapalli, N.; Chénard, E.; Sevov, C. S.; Prendergast, D.; Moore, J. S.; Helms, B. A. Macromolecular Design Strategies for Preventing Active-Material Crossover in Non-Aqueous All-Organic Redox-Flow Batteries. *Angew. Chem., Int. Ed.* **2017**, *56*, 1595−1599.
(14) De La Garza, G. D.; Kaur, A. P.; Shkrob, I. A.; Robertson, L. A.; Odom, S. A.; McNeil, A. J. Soluble and Stable Symmetric Tetrazines as Anolytes in Redox Flow Batteries. *J. Mater. Chem. A* **2022**, *10*, 18745−18752.
(15) Kim, D.; Sanford, M. S.; Vaid, T. P.; McNeil, A. J. A Nonaqueous Redox-Matched Flow Battery with Charge Storage in Insoluble Polymer Beads. *Chem.—Eur. J.* **2022**, *28*, No. e202200149.
(16) Nagarjuna, G.; Hui, J.; Cheng, K. J.; Lichtenstein, T.; Shen, M.; Moore, J. S.; Rodríguez-López, J. Impact of Redox-Active Polymer Molecular Weight on the Electrochemical Properties and Transport Across Porous Separators in Nonaqueous Solvents. *J. Am. Chem. Soc.* **2014**, *136*, 16309−16316.
(17) Duan, W.; Huang, J.; Kowalski, J. A.; Shkrob, I. A.; Vijayakumar, M.; Walter, E.; Pan, B.; Yang, Z.; Milshtein, J. D.; Li, B.; Liao, C.; Zhang, Z.; Wang, W.; Liu, J.; Moore, J. S.; Brushett, F. R.; Zhang, L.; Wei, X. "Wine-Dark Sea" in an Organic Flow Battery: Storing Negative Charge in 2,1,3-Benzothiadiazole Radicals Leads to Improved Cyclability. *ACS Energy Lett.* **2017**, *2*, 1156−1161.
(18) Wei, X.; Duan, W.; Huang, J.; Zhang, L.; Li, B.; Reed, D.; Xu, W.; Sprenkle, V.; Wang, W. A High-Current, Stable Nonaqueous Organic Redox Flow Battery. *ACS Energy Lett.* **2016**, *1*, 705−711.
(19) You, W.; Noonan, K. J. T.; Coates, G. W. Alkaline-Stable Anion Exchange Membranes: A Review of Synthetic Approaches. *Prog. Polym. Sci.* **2020**, *100*, 101177.
(20) Zeng, L.; Zhao, T. S.; Wei, L.; Jiang, H. R.; Wu, M. C. Anion Exchange Membranes for Aqueous Acid-Based Redox Flow Batteries: Current Status and Challenges. *Appl. Energy* **2019**, *233*−*234*, 622−643.
(21) Du, N.; Roy, C.; Peach, R.; Turnbull, M.; Thiele, S.; Bock, C. Anion-Exchange Membrane Water Electrolyzers. *Chem. Rev.* **2022**, *122*, 11830−11895.
(22) Jett, B.; Flynn, A.; Sigman, M. S.; Sanford, M. S. Identifying Structure-Function Relationships to Modulate Crossover in Non-aqueous Redox Flow Batteries. *J. Mater. Chem. A* **2023**, *11*, 22288−22294.
(23) Matsuda, Y.; Tanaka, K.; Okada, M.; Takasu, Y.; Morita, M.; Matsumura-Inoue, T. A Rechargeable Redox Battery Utilizing Ruthenium Complexes with Non-Aqueous Organic Electrolyte. *J. Appl. Electrochem.* **1988**, *18*, 909−914.
(24) Liu, Q.; Sleightholme, A. E. S.; Shinkle, A. A.; Li, Y.; Thompson, L. T. Non-Aqueous Vanadium Acetylacetonate Electrolyte for Redox Flow Batteries. *Electrochem. Commun.* **2009**, *11*, 2312−2315.
(25) Mun, J.; Lee, M.-J.; Park, J.-W.; Oh, D.-J.; Lee, D.-Y.; Doo, S.-G. Non-Aqueous Redox Flow Batteries with Nickel and Iron Tris(2,2′-Bipyridine) Complex Electrolyte. *Electrochem. Solid-State Lett.* **2012**, *15*, A80.
(26) Shin, S.-H.; Yun, S.-H.; Moon, S.-H. A Review of Current Developments in Non-Aqueous Redox Flow Batteries: Characterization of Their Membranes for Design Perspective. *RSC Adv.* **2013**, *3*, 9095−9116.
(27) Robinson, S. G.; Yan, Y.; Hendriks, K. H.; Sanford, M. S.; Sigman, M. S. Developing a Predictive Solubility Model for Monomeric and Oligomeric Cyclopropenium-Based Flow Battery Catholytes. *J. Am. Chem. Soc.* **2019**, *141*, 10171−10176.
(28) Shrestha, A.; Hendriks, K. H.; Sigman, M. S.; Minteer, S. D.; Sanford, M. S. Realization of an Asymmetric Non-Aqueous Redox Flow Battery through Molecular Design to Minimize Active Species Crossover and Decomposition. *Chem.—Eur. J.* **2020**, *26*, 5369−5373.
(29) Yan, Y.; Robinson, S. G.; Sigman, M. S.; Sanford, M. S. Mechanism-Based Design of a High-Potential Catholyte Enables a 3.2 V All-Organic Nonaqueous Redox Flow Battery. *J. Am. Chem. Soc.* **2019**, *141*, 15301−15306.
(30) Montoto, E. C.; Nagarjuna, G.; Moore, J. S.; Rodríguez-López, J. Redox Active Polymers for Non-Aqueous Redox Flow Batteries: Validation of the Size-Exclusion Approach. *J. Electrochem. Soc.* **2017**, *164*, A1688−A1694.
(31) Yan, Y.; Sitaula, P.; Odom, S. A.; Vaid, T. P. High Energy Density, Asymmetric, Nonaqueous Redox Flow Batteries without a Supporting Electrolyte. *ACS Appl. Mater. Interfaces* **2022**, *14*, 49633−49640.
(32) Ahn, S.; Jang, J. H.; Kang, J.; Na, M.; Seo, J.; Singh, V.; Joo, J. M.; Byon, H. R. Systematic Designs of Dicationic Heteroarylpyridiniums as Negolytes for Nonaqueous Redox Flow Batteries. *ACS Energy Lett.* **2021**, *6*, 3390−3397.
(33) Daub, N.; Hendriks, K. H.; Janssen, R. A. J. Two-Electron Tetrathiafulvalene Catholytes for Nonaqueous Redox Flow Batteries. *Batteries Supercaps* **2022**, *5*, No. e202200386.
(34) Krivina, R. A.; Lindquist, G. A.; Yang, M. C.; Cook, A. K.; Hendon, C. H.; Motz, A. R.; Capuano, C.; Ayers, K. E.; Hutchison, J. E.; Boettcher, S. W. Three-Electrode Study of Electrochemical Ionomer Degradation Relevant to Anion-Exchange-Membrane Water Electrolyzers. *ACS Appl. Mater. Interfaces* **2022**, *14*, 18261−18274.
(35) Hudak, N. S.; Small, L. J.; Pratt, H. D.; Anderson, T. M. Through-Plane Conductivities of Membranes for Nonaqueous Redox Flow Batteries. *J. Electrochem. Soc.* **2015**, *162*, A2188−A2194.
(36) Liang, Z.; Attanayake, N. H.; Greco, K. V.; Neyhouse, B. J.; Barton, J. L.; Kaur, A. P.; Eubanks, W. L.; Brushett, F. R.; Landon, J.; Odom, S. A. Comparison of Separators vs Membranes in Nonaqueous Redox Flow Battery Electrolytes Containing Small Molecule Active Materials. *ACS Appl. Energy Mater.* **2021**, *4*, 5443−5451.
(37) Mushtaq, K.; Lagarteira, T.; Zaidi, A. A.; Mendes, A. *In-Situ* Crossover Diagnostics to Assess Membrane Efficacy for Non-Aqueous Redox Flow Battery. *J. Energy Storage* **2021**, *40*, 102713.
(38) George, T. Y.; Thomas, I. C.; Haya, N. O.; Deneen, J. P.; Wang, C.; Aziz, M. J. Membrane-Electrolyte System Approach to Understanding Ionic Conductivity and Crossover in Alkaline Flow Cells. *ACS Appl. Mater. Interfaces* **2023**, *15*, 57252−57264.
(39) Cassady, H. J.; Yang, Z.; Rochow, M. F.; Saraidaridis, J. D.; Hickner, M. A. Crossover Flux and Ionic Resistance Metrics in Polysulfide-Permanganate Redox Flow Battery Membranes. *J. Electrochem. Soc.* **2024**, *171*, 030527.
(40) Lehmann, M. L.; Tyler, L.; Self, E. C.; Yang, G.; Nanda, J.; Saito, T. Membrane Design for Non-Aqueous Redox Flow Batteries: Current Status and Path Forward. *Chem* **2022**, *8*, 1611−1636.
(41) Gong, K.; Fang, Q.; Gu, S.; Li, S. F. Y.; Yan, Y. Nonaqueous Redox-Flow Batteries: Organic Solvents, Supporting Electrolytes, and Redox Pairs. *Energy Environ. Sci.* **2015**, *8*, 3515−3530.
(42) Alder, C. M.; Hayler, J. D.; Henderson, R. K.; Redman, A. M.; Shukla, L.; Shuster, L. E.; Sneddon, H. F. Updating and Further Expanding GSK's Solvent Sustainability Guide. *Green Chem.* **2016**, *18*, 3879−3890.
(43) The hydrodynamic radii are approximated with the Stokes-Einstein equation, wherein the radius is inversely proportional to the diffusion coefficient of the molecule in solution (diffusion coefficients are calculated in SI Table S8) and solution viscosity, which is primarily affected by the solvent and excess supporting electrolyte. See ref: Berkowicz, S.; Perakis, F. Exploring the Validity of the Stokes-Einstein Relation in Supercooled Water Using Nanomolecular Probes. *Phys. Chem. Chem. Phys.* **2021**, *23*,*23*, 25490−25499.

https://doi.org/10.1021/acsami.4c07026
ACS Appl. Mater. Interfaces 2024, 16, 53643−53651

(44) Li, M.; Odom, S. A.; Pancoast, A. R.; Robertson, L. A.; Vaid, T. P.; Agarwal, G.; Doan, H. A.; Wang, Y.; Suduwella, T. M.; Bheemireddy, S. R.; Ewoldt, R. H.; Assary, R. S.; Zhang, L.; Sigman, M. S.; Minteer, S. D. Experimental Protocols for Studying Organic Non-Aqueous Redox Flow Batteries. *ACS Energy Lett.* **2021**, *6*, 3932−3943.
(45) Gandomi, Y. A.; Aaron, D. S.; Houser, J. R.; Daugherty, M. C.; Clement, J. T.; Pezeshki, A. M.; Ertugrul, T. Y.; Moseley, D. P.; Mench, M. M. Critical Review—Experimental Diagnostics and Material Characterization Techniques Used on Redox Flow Batteries. *J. Electrochem. Soc.* **2018**, *165*, A970−A1010.
(46) Adams & Chittenden Scientific Glass Coop Home Page. https://adamschittenden.com/ (accessed 2024/02/09).
(47) Bard, A. J.; Faulkner, L. R. *Electrochemical Methods: Fundamentals and Applications*; John Wiley and Sons, Inc.: US, 2001; pp 230−243.
(48) Wang, H.; Sayed, S. Y.; Luber, E. J.; Olsen, B. C.; Shirurkar, S. M.; Venkatakrishnan, S.; Tefashe, U. M.; Farquhar, A. K.; Smotkin, E. S.; McCreery, R. L.; Buriak, J. M. Redox Flow Batteries: How to Determine Electrochemical Kinetic Parameters. *ACS Nano* **2020**, *14*, 2575−2584.
(49) Yang, Z.; Tong, L.; Tabor, D. P.; Beh, E. S.; Goulet, M.-A.; De Porcellinis, D.; Aspuru-Guzik, A.; Gordon, R. G.; Aziz, M. J. Alkaline Benzoquinone Aqueous Flow Battery for Large-Scale Storage of Electrical Energy. *Adv. Energy Mater.* **2018**, *8*, 1702056.
(50) Díaz, J. C.; Kitto, D.; Kamcev, J. Accurately Measuring the Ionic Conductivity of Membranes via the Direct Contact Method. *J. Membr. Sci.* **2023**, *669*, 121304.
(51) Fong, K. D.; Self, J.; Diederichsen, K. M.; Wood, B. M.; McCloskey, B. D.; Persson, K. A. Ion Transport and the True Transference Number in Nonaqueous Polyelectrolyte Solutions for Lithium-ion Batteries. *ACS Cent. Sci.* **2019**, *5*, 1250−1260.
(52) Ford, H. O.; Park, B.; Jiang, J.; Seidler, M. E.; Schaefer, J. L. Enhanced Li^+ Conduction within Single-ion Conducting Polymer Gel Electrolytes via Reduced Cation-Polymer Interaction. *ACS Mater. Lett.* **2020**, *2*, 272−279.
(53) Su, L.; Darling, R. M.; Gallagher, K. G.; Xie, W.; Thelen, J. L.; Badel, A. F.; Barton, J. L.; Cheng, K. J.; Balsara, N. P.; Moore, J. S.; Brushett, F. R. An Investigation of the Ionic Conductivity and Species Crossover of Lithiated Nafion 117 in Nonaqueous Electrolytes. *J. Electrochem. Soc.* **2016**, *163*, A5253−A5262.
(54) Darling, R.; Gallagher, K.; Xie, W.; Su, L.; Brushett, F. Transport Property Requirements for Flow Battery Separators. *J. Electrochem. Soc.* **2016**, *163*, A5029−A5040.
(55) Kong, T.; Li, J.; Wang, W.; Zhou, X.; Xie, Y.; Ma, J.; Li, X.; Wang, Y. Enabling Long-Life Aqueous Organic Redox Flow Batteries with a Highly Stable, Low Redox Potential Phenazine Anolyte. *ACS Appl. Mater. Interfaces* **2024**, *16*, 752−760.
(56) Modak, S. V.; Shen, W.; Singh, S.; Herrera, D.; Oudeif, F.; Goldsmith, B. R.; Huan, X.; Kwabi, D. G. Understanding Capacity Fade in Organic Redox-Flow Batteries by Combining Spectroscopy with Statistical Inference Techniques. *Nat. Commun.* **2023**, *14*, 3602.
(57) Small, L. J.; Pratt, H. D., III; Anderson, T. M. Crossover in Membranes for Aqueous Soluble Organic Redox Flow Batteries. *J. Electrochem. Soc.* **2019**, *166*, A2536−A2542.
(58) Neyhouse, B. J.; Brushett, F. R. A Spreadsheet-based Redox Flow Battery Cell Cycling Model enabled by Closed-form Approximations. *J. Electrochem. Soc.* **2024**, *171*, 080518.
(59) Jacquemond, R. R.; Geveling, R.; Forner-Cuenca, A.; Nijmeijer, K. On the Characterization of Membrane Transport Phenomena and Ion Exchange Capacity for Non-Aqueous Redox Flow Batteries. *J. Electrochem. Soc.* **2022**, *169*, 080528.
(60) Geise, G. M.; Paul, D. R.; Freeman, B. D. Fundamental Water and Salt Transport Properties of Polymeric Materials. *Prog. Polym. Sci.* **2014**, *39*, 1−42.
(61) Machado, C. A.; Brown, G. O.; Yang, R.; Hopkins, T. E.; Pribyl, J. G.; Epps, T. H., III Redox Flow Battery Membranes: Improving Battery Performance by Leveraging Structure−Property Relationships. *ACS Energy Lett.* **2021**, *6*, 158−176.
(62) Darling, R. M.; Saraidaridis, J. D.; Shovlin, C.; Fortin, M. The Influence of Current Density on Transport of Vanadium Acetylacetonate through a Cation-Exchange Membrane. *J. Electrochem. Soc.* **2022**, *169*, 030514.
(63) Neyhouse, B. J.; Darling, R. M.; Saraidaridis, J. D.; Brushett, F. R. A Method for Quantifying Crossover in Redox Flow Cells through Compositionally Unbalanced Symmetric Cell Cycling. *J. Electrochem. Soc.* **2023**, *170*, 080514.
(64) Fenton, A. M., Jr; Jha, R. K.; Neyhouse, B. J.; Kaur, A. P.; Dailey, D. A.; Odom, S. A.; Brushett, F. R. On the Challenges of Materials and Electrochemical Characterization of Concentrated Electrolytes for Redox Flow Batteries. *J. Mater. Chem. A* **2022**, *10*, 17988−17999.
(65) Peltier, C. R.; Rhodes, Z.; Macbeth, A. J.; Milam, A.; Carroll, E.; Coates, G. W.; Minteer, S. D. Suppressing Crossover in Nonaqueous Redox Flow Batteries with Polyethylene-Based Anion-Exchange Membranes. *ACS Energy Lett.* **2022**, *7*, 4118−4128.
(66) Mazumder, Md. M. R.; Jadhav, R. G.; Minteer, S. D. Phenyl Acrylate-Based Cross-Linked Anion Exchange Membranes for Non-Aqueous Redox Flow Batteries. *ACS Mater. Au* **2023**, *3*, 557−568.
(67) Li, Y.; Sniekers, J.; Malaquias, J. C.; Van Goethem, C.; Binnemans, K.; Fransaer, J.; Vankelecom, I. F. J. Crosslinked Anion Exchange Membranes Prepared from Poly(phenylene oxide) (PPO) for Non-Aqueous Redox Flow Batteries. *J. Power Sources* **2018**, *378*, 338−344.
(68) Mandal, M.; Huang, G.; Hassan, N. U.; Mustain, W. E.; Kohl, P. A. Poly(norbornene) Anion Conductive Membranes: Homopolymer, Block Copolymer and Random Copolymer Properties and Performance. *J. Mater. Chem. A* **2020**, *8*, 17568−17578.

https://doi.org/10.1021/acsami.4c07026
ACS Appl. Mater. Interfaces 2024, 16, 53643−53651